# Enhanced Ambipolar Charge Injection with Semiconducting Polymer/Carbon Nanotube Thin Films for Light-Emitting Transistors

**Michael C. Gwinner,[†,§] Florian Jakubka,[‡,§] Florentina Gannott,[‡] Henning Sirringhaus,[†] and Jana Zaumseil[‡,*]**

[†]Cavendish Laboratory, University of Cambridge, JJ Thomson Avenue, Cambridge CB3 0HE, United Kingdom and [‡]Institute of Polymer Materials, Friedrich-Alexander University Erlangen-Nuremberg, Martensstrasse 7, D-91058 Erlangen, Germany. [§]These authors contributed equally to this work.

## ABSTRACT

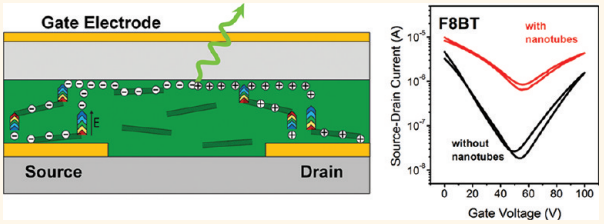


We investigate the influence of small amounts of semiconducting single-walled carbon nanotubes (SWNTs) dispersed in polyfluorenes such as poly(9,9-di-*n*-octylfluorene-*alt*-benzothiadiazole (F8BT) and poly(9,9-dioctylfluorene) (F8) on device characteristics of bottom contact/top gate ambipolar light-emitting field-effect transistors (LEFETs) based on these conjugated polymers. We find that the presence of SWNTs within the semiconducting layer at concentrations below the percolation limit significantly increases both hole and electron injection, even for a large band gap semiconductor like F8, without leading to significant luminescence quenching of the conjugated polymer. As a result of the reduced contact resistance and lower threshold voltages, larger ambipolar currents and thus brighter light emission are observed. We examine possible mechanisms of this effect such as energy level alignment, reduced bulk resistance above the contacts, and field-enhanced injection at the nanotube tips. The observed ambipolar injection improvement is applicable to most conjugated polymers in staggered transistor configurations or similar organic electronic devices where injection barriers are an issue.

**KEYWORDS:** single-walled carbon nanotubes · semiconducting polymers · ambipolar · field-effect transistor · light-emitting · charge injection

Efficient injection of charge carriers is crucial for organic electronic devices such as organic light-emitting diodes (OLEDs) and field-effect transistors (OFETs) with applications in flexible electronics. Large injection barriers and high contact resistance increase operating voltages and power dissipation and thus reduce device efficiency. Depending on the position of the HOMO/LUMO levels of a particular organic semiconductor, the work function of the injecting electrode has to be chosen or adjusted according to whether holes or electrons are to be injected.[1,2] In the case of ambipolar OFETs for complementary circuits[3] and light-emitting field-effect transistors (LEFETs),[4] equally efficient injection of holes and electrons is required. Due to the large band gap of most organic semiconductors (2−3 eV), it is not possible to find one metal that results in a low Schottky barrier for both polarities of charge carriers. This fundamental issue has been addressed in several ways over the past few years. The straightforward approach is to use two different metals: a high work function metal for hole injection (*e.g.*, Au, Pd) and a low work function metal (*e.g.*, Ca, Mg, Al) for electron injection similar to an OLED.[5,6] However, low work function metals are not air-stable, and patterning is limited to shadow masking. Both of these severely reduce the applicability of such devices. Recently, ZnO was introduced as a possible air-stable injection layer for electrons in polymer OFETs but had to be photolithographically patterned in a separate step.[7] Self-assembled monolayers of thiols are able to change the injection barrier of gold for both holes and electrons depending on their dipole moment.[8−11] This method is widely applicable except for semiconductors that require high-temperature post-deposition annealing for best performance or alignment, for example, high molecular weight conjugated polymers. During heating, the thiol molecules desorb from the surface and the intended effect is lost. Furthermore, this method can only be applied to gold and silver electrodes, which are not the best choice for organic electronics

* Address correspondence to jana.zaumseil@ww.uni-erlangen.de.

Received for review October 8, 2011 and accepted December 5, 2011.

**Published online December 05, 2011**
10.1021/nn203874a

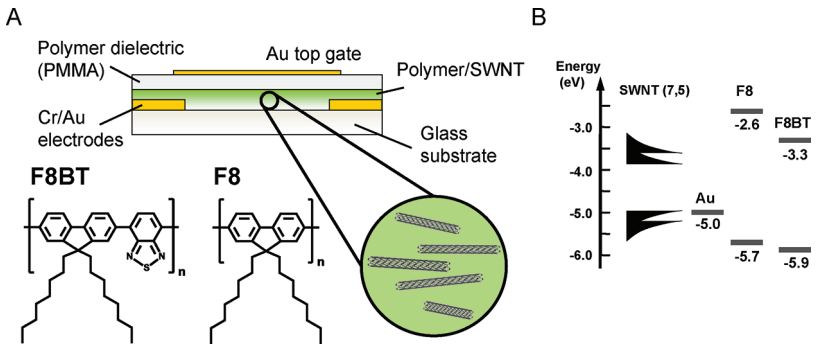


**Figure 1. (A) Schematic illustration of bottom contact/top gate polymer field-effect transistor with carbon nanotubes dispersed in the semiconducting polymers F8BT and F8. (B) Energy level diagram of a semiconducting SWNT with (7,5) chirality according to Tanaka *et al.*,[32] gold (injecting electrode) and HOMO/LUMO levels of both F8 and F8BT.**

in general. It is also difficult to deposit different self-assembled monolayers for hole and electron injection on the source and drain electrodes without additional photolithography steps.

The device configuration also has an impact on charge injection and contact resistance. The staggered or bottom contact/top gate configuration (as shown in Figure 1A) universally shows lower contact resistance than a coplanar OFET using the same electrode and semiconducting material.[12,13] The overlap of the gate electrode with the source–drain electrodes and the applied gate field support injection of charges even when a high injection barrier is present. However, since all charge carriers have to travel through the undoped polymer film of low conductivity to reach the interface with the dielectric and enter the charge accumulation layer, the contact resistance increases again with film thickness.[14] The staggered configuration is a very common and convenient structure especially for all printed OFETs. The reduced contact resistance in staggered devices was previously exploited for an ambipolar LEFET based on poly(9,9-di-*n*-octylfluorene-*alt*-benzothiadiazole (F8BT).[15,16] In an ambipolar light-emitting FET, holes and electrons are injected into the channel from the source and drain, respectively, depending on the applied voltages. They form accumulation layers that extend from the corresponding electrodes and meet within the channel where holes and electrons recombine and result in light emission. The position of this narrow emission zone depends on the applied voltages. As a first approximation, an ambipolar transistor can be modeled as a saturated hole and electron channel in series, assuming that all charge carriers recombine.[4] The conjugated polymer F8BT, used in this study, is an efficient green emitter (photoluminescence efficiency ~60%) but has a large band gap of 2.6 eV (Figure 1B). The injection barriers for holes and electrons are about 1.2 eV, and thus no injection is found for coplanar devices with gold electrodes. However, using a bottom contact/top gate structure enables ambipolar charge injection. However, even in this configuration, the high injection barrier leads to very high, non-ohmic contact resistance. Reducing this contact resistance would lead to a lower potential drop and thus less power dissipation at the contacts, higher ambipolar currents at lower applied voltages, and higher maximum brightness. Both self-assembled monolayers and ZnO for electron injection were previously employed to lower contact resistance in this device structure with some success, but hole and electron injection could not be improved equally.[7,10,11] The drawbacks of the previously applied methods for reducing contact resistance demonstrate that there is a need for a novel and easy-to-implement method that allows us to increase charge injection of both charge carriers.

Here we report a simple method that significantly improves the injection of both holes and electrons into large band gap polyfluorenes such as F8BT and the blue-emitting poly(9,9-dioctylfluorene) (F8) (see Figure 1A) in a bottom contact/top gate FET structure by adding small amounts of single-walled carbon nanotubes (SWNTs) to the semiconducting polymer without creating percolation paths between the source–drain electrodes. This method does not require any additional patterning steps and is compatible with high- and low-temperature processing. It leads to lower contact resistance and thus lower threshold/onset voltages for both holes and electrons at the same time and higher ambipolar currents and emission intensities.

Carbon nanotubes have been of interest for charge injection in organic electronics for some time. Several groups have reported examples of injecting electrodes for OFETs where the main electrode material was a metal or conducting polymer and carbon nanotubes extended from the edge of the electrode laterally into the channel.[17–19] Others used patterned conducting films of carbon nanotubes directly as the injecting electrodes.[20,21] Most devices with carbon nanotubes showed lower contact resistance than devices based on gold electrodes. However, all of these examples used bottom contact/bottom gate configurations (coplanar). That is, charge was injected laterally into the accumulation channel with the lateral field acting along the length of the nanotubes. In a bottom

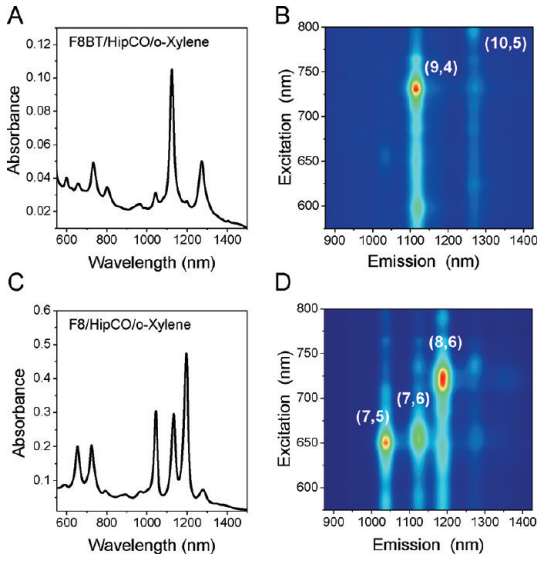


**Figure 2. Absorption spectra of HipCO nanotubes dispersed in F8BT/*o*-xylene (A) and F8/*o*-xylene (C) after centrifugation. Excitation–emission maps for photoluminescence from these dispersions F8BT/HipCO (B) and F8/HipCO (D). Predominant types of SWNTs are labeled.**

contact/top gate structure, as shown in Figure 1A, charges are injected vertically into the polymer layer assisted by the gate field. The only reported carbon nanotube electrode device that also features this vertical injection is the so-called carbon nanotube enabled vertical field-effect transistor (CN-VFET) that uses a conducting carbon nanotube network as a porous source electrode.[22,23]

Conjugated polymers are known for efficiently dispersing carbon nanotubes in organic solvents. Solutions based on polythiophenes and polyphenylvinylenes that disperse SWNTs nonselectively at high concentrations were used to fabricate hybrid solar cells using the nanotubes for electron transport.[24,25] Certain polyfluorenes, however, can selectively wrap around semiconducting SWNTs of a particular chirality or diameter.[26,27] After sonication and centrifugation of a polyfluorene solution with HipCO carbon nanotube powder that contains a broad distribution of metallic and semiconducting nanotubes, only completely debundled semiconducting SWNTs remain in dispersion. The amount and type of SWNT depends on the polymer and the dispersion solvent. F8BT solutions are generally selective for (9,4) and (10,5) SWNTs, while F8 solutions are selective for SWNTs with large chiral angles, for example, chiralities (8,6), (7,5), (7,6), and (8,7). The absorption spectra and excitation–emission maps in Figure 2 show the distribution of dispersed nanotubes for the polymers and solvents used in this study. Note that unlike previous studies we are using conjugated polymers with rather high molecular weights that are necessary to obtain high-performance FETs.[28] During sonication, the molecular weight, in particular the high molecular weight tail of the polymers, is reduced slightly (see Methods and S1 of Supporting Information). The concentration of nanotubes after centrifugation at 60 000*g* is low and depends on the polymer. Using a recently published carbon absorption cross section of $1.7 \times 10^{-17}$ cm$^2$ for the $E_{11}$ absorption peaks,[29] we estimate approximately 0.001 mg/mL SWNTs in F8/*o*-xylene solutions and 0.0002 mg/mL SWNT in F8BT/*o*-xylene solutions from the absorption spectra in Figure 2A,C. In both cases, spin-coating a thin film of 50–70 nm (after adding pristine polymer to achieve the desired film thickness) on top of prepatterned gold source–drain electrodes with a channel length of 20 $\mu$m does not lead to any direct percolation paths of the nanotubes or any significantly increased film conductivity that would indicate a continuous SWNT network.

The completed field-effect transistors with PMMA (500 nm) as the gate dielectric and evaporated gold top gate electrodes showed markedly improved device characteristics compared to FETs with pure semiconducting polymer layers processed in the same way. Figure 3 shows the transfer and output characteristics of ambipolar F8BT LEFETs with and without HipCO nanotubes. As extracted from Figure 3A,B, the onset voltage for holes drops from −22 V without SWNTs to −12 V with SWNTs, while the electron onset voltages are also reduced from 28 to 12 V. In both cases, the current onsets at low source–drain voltages also become much steeper. The observed reduction in onset voltages for electron and hole transport are at least partially due to lower contact resistance. The source–drain currents at low source–drain voltages in the output characteristics, plotted in Figure 3C,D, are significantly larger in devices with SWNTs than in those without, indicating substantially lower, yet still non-ohmic, contact resistance. Gated four-point probe measurements of FETs with and without SWNTs indicate a reduction of contact resistance by at least an order of magnitude for hole and electron injection (see S2).

While the SWNTs have the effect of lowering threshold/onset voltages (see Table 1), the effective saturation mobilities for both carriers are also slightly reduced to $1 \times 10^{-3}$ cm$^2$ V$^{-1}$ s$^{-1}$ for holes and $0.5 \times 10^{-3}$ cm$^2$ V$^{-1}$ s$^{-1}$ for electrons. Together with the low off-currents, this indicates again that there are no SWNT percolation paths. According to the energy level diagram of semiconducting SWNTs and F8BT (see Figure 1B), the nanotubes might even act as shallow traps, which could explain the lower mobilities. Due to the reduced onset voltages, the ambipolar currents and thus overall brightness of light emission are 2 orders of magnitude larger for LEFETs with SWNTs. At the same time, the external quantum efficiency (EQE) measured with a silicon photodiode in the forward direction through the semitransparent gate electrode and plotted in Figure 3E is similar to the best pure F8BT devices (note that using this method we do not obtain

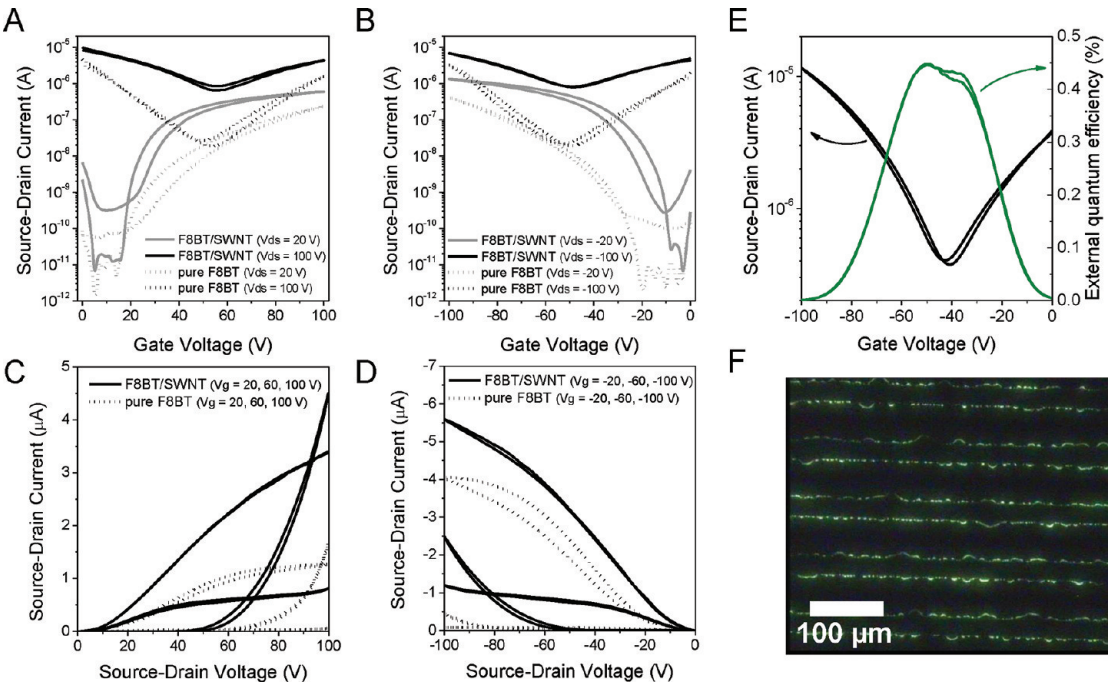


**Figure 3. Comparison of transfer (A,B) and output characteristics (C,D) at positive and negative gate voltages of LEFETs with pure F8BT (dotted lines) and F8BT/HipCO (solid lines) films ($L$ = 20 $\mu$m, $W/L$ = 1000, $C_i$ = 4.4 nF cm$^{-2}$). (E) Current−voltage characteristics and external quantum efficiency of green light emission (maximum at 560 nm) from LEFETs with F8BT/HipCO thin films ($V_{ds}$ = −100 V, $L$ = 20 $\mu$m, $W/L$ = 1000, $C_i$ = 4.4 nF cm$^{-2}$). (F) Optical micrograph of visible light emission from LEFET with interdigitated electrodes during a transfer scan.**

**TABLE 1. Average Device Parameters of Polymer FETs Processed under the Same Conditions with and without Added SWNT**

| | saturation hole mobility ($cm^2 V^{-1} s^{-1}$) | saturation electron mobility ($cm^2 V^{-1} s^{-1}$) | onset voltage holes (V) | onset voltage electrons (V) |
|---|---|---|---|---|
| F8BT pure | $(1.8 \pm 0.3) \times 10^{-3}$ | $(0.7 \pm 0.04) \times 10^{-3}$ | $-22 \pm 5$ | $28 \pm 7$ |
| F8BT/HipCO | $(1.1 \pm 0.2) \times 10^{-3}$ | $(0.5 \pm 0.08) \times 10^{-3}$ | $-12 \pm 5$ | $12 \pm 5$ |
| F8BT pure with SWNT electrodes | $(1.3 \pm 0.1) \times 10^{-3}$ | $(0.7 \pm 0.1) \times 10^{-3}$ | $-16 \pm 4$ | $20 \pm 4$ |
| F8 pure | $(0.18 \pm 0.03) \times 10^{-3}$ | $(0.03 \pm 0.02) \times 10^{-3}$ | $-21 \pm 6$ | $52 \pm 8$ |
| F8/HipCO | $(0.3 \pm 0.05) \times 10^{-3}$ | $(0.86 \pm 0.3) \times 10^{-3}$ | $0 \pm 8$ | $26 \pm 5$ |

an absolute value of the EQE as not all of the emitted photons but just the small fraction transmitted through the gold gate are collected[16]). Possible energy transfer from the polymer to the nanotubes that emit near-infrared light[30] is currently being investigated, but clearly, the limited amount of nanotubes does not quench the visible F8BT emission significantly. Figure 3F shows an optical micrograph of the green emission zone of the LEFETs in the ambipolar regime.

The described improved device characteristics are apparent not only for devices that were annealed to the liquid crystalline melt of F8BT (290 °C, see Figure 3), which is the standard procedure, but also for films annealed below the glass transition temperature at 150 °C (S3). Previously, it was difficult to achieve acceptable charge injection into F8BT without annealing to high temperatures. This is important for devices with semiconducting films that should remain amorphous, for example, for optical waveguiding applications.[31]

The effect of enhanced charge injection is even more dramatic for LEFETs with F8 as the semiconductor. Its large band gap (3.1 eV) and low electron affinity of −2.6 eV make electron injection from gold very unfavorable. The device characteristics for pure F8 FETs, shown in Figure 4A,B, exhibit almost no electron transport or only with very large onset voltages and hysteresis. Previously, we improved the electron injection into F8 with an additional ZnO layer on one electrode, but even then, onset voltages and hysteresis remained quite large.[7] For devices fabricated from F8/HipCO dispersions, electron injection and transport become observable in the transfer and output characteristics (Figure 4A−D). The electron onset decreases from values above 52 V to about 25 V. The output characteristics for negative voltages (Figure 4C) show reasonably good injection of holes into pure F8 from gold, which is expected as the HOMO level of F8 is closer to the gold work function than in the case of

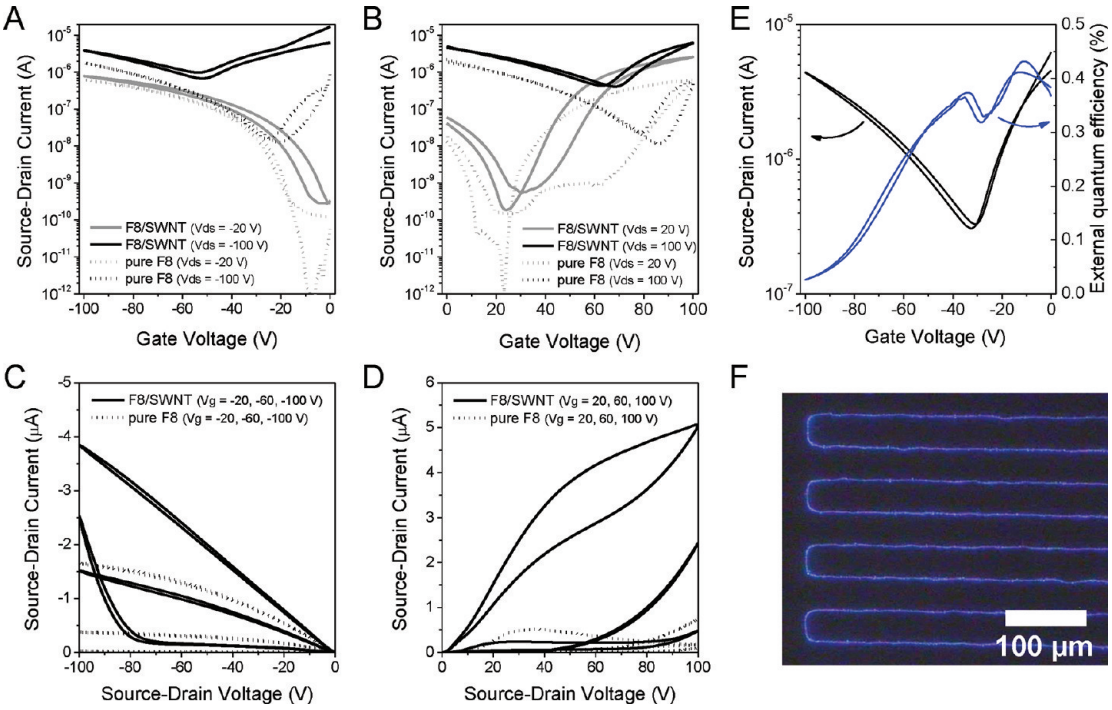


**Figure 4. Comparison of transfer (A,B) and output characteristics (C,D) at negative and positive gate voltages of FETs with pure F8 (dotted lines) and F8/HipCO (solid lines) films ($L$ = 20 $\mu$m, $W/L$ = 1000, $C_i$ = 4.4 nF cm$^{-2}$). (E) Current–voltage characteristics and external quantum efficiency of blue light emission (maximum at 433 nm) from LEFETs with F8/HipCO thin films ($V_{ds}$ = −100 V, $L$ = 20 $\mu$m, $W/L$ = 1000, $C_i$ = 4.4 nF cm$^{-2}$). (F) Optical micrograph of visible light emission from LEFET with interdigitated electrodes during a transfer scan.**

F8BT (see Figure 1B). Nevertheless, even in this case, the added nanotubes lead to improved current–voltage characteristics. The onset for hole transport is reduced from about −21 to 0 V or even slightly positive voltages, and the source–drain current at low source–drain voltages increases almost linearly. Similar to the F8BT devices, the hole and electron mobilities remain largely unchanged. For F8/SWNT devices, higher electron than hole mobilities are found (Table 1), while for FETs without SWNTs, current and voltage hysteresis and large threshold voltages are a source of error for calculated electron mobilities. Previously unattainable high ambipolar currents and bright, stable blue light emission can be achieved with F8/HipCO blends (see Figure 4E,F), exhibiting good external quantum efficiencies. Note that despite the approximately five times higher concentration of SWNTs in F8 compared to F8BT the off-currents are still low.

Clearly the presence of SWNTs has a substantial effect on injection of charges into semiconducting polymers. To test the limit of this effect, we wanted to increase the concentration of nanotubes at the contacts without causing percolation paths in the channel. We chose to use spin-cast semiconducting CoMoCat nanotubes that contain mainly semiconducting SWNTs similar to the polymer blends as an injecting layer. Purified and well-dispersed CoMoCat-SWNTs were spin-coated from 1,2-dichlorobenzene onto substrates with prepatterned gold electrodes (see Figure 5A), forming a dense conducting layer. Subsequently, all nanotubes were removed from the channel region by photolithography with an inverse mask and oxygen plasma, thus leaving SWNTs only on top of the gold electrodes. Spin-coating pure F8BT as the active layer and PMMA as the dielectric followed by thermal evaporation of the gate electrode completed the devices as described before. The resulting transfer characteristics of these FETs show similar behavior to the F8BT/HipCO blend FETs with low onset voltages and little hysteresis. The effective hole and electron mobilities are again similar to those of F8BT without carbon nanotubes (see Table 1), indicating that charge transport through the channel is not affected and no nanotubes remained in the channel. Due to the significantly lower onset voltages for both holes and electrons of −16 and 20 V, respectively, compared to devices with bare gold electrodes, the LEFETs with SWNT electrodes exhibit very high ambipolar currents and bright light emission, as shown in Figure 5C,D. Remarkably, however, the output characteristics feature almost ohmic charge injection for both holes and electrons as indicated by the near linear drain–current increase at low source–drain voltages (see Figure 5E,F). The contact resistance for both holes and electrons is decreased to values similar to polymers whose HOMO/LUMO levels are aligned with the injecting metal work function. Similarly, good charge injection into F8BT could previously only be achieved for

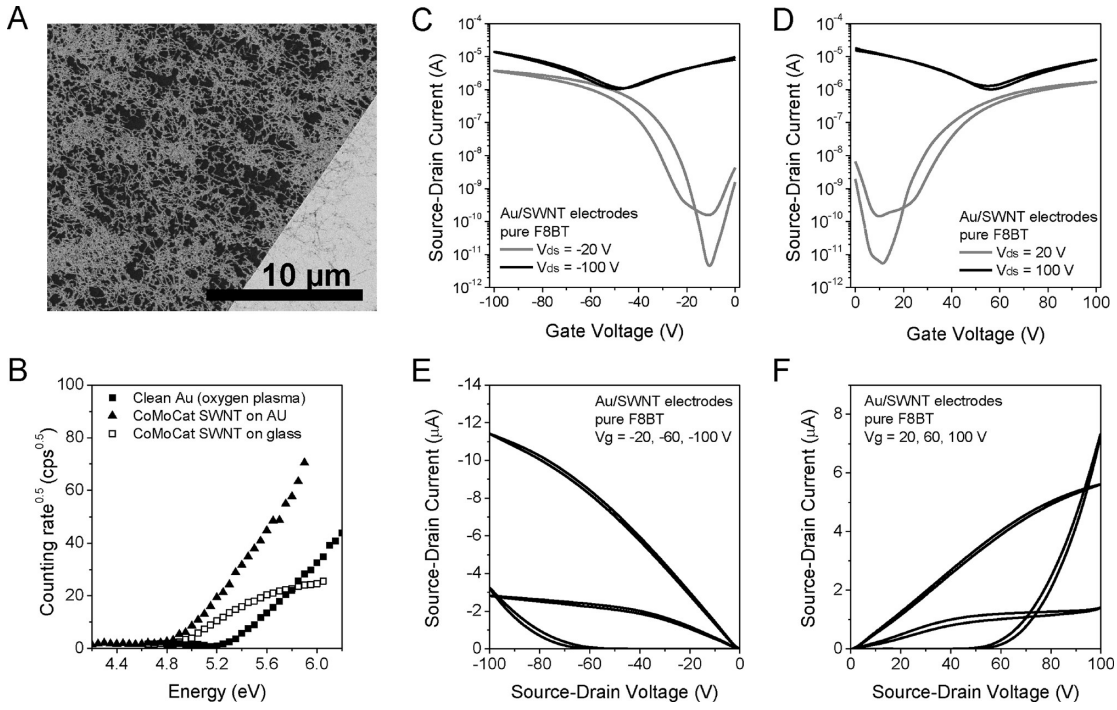


**Figure 5. (A) Scanning electron micrograph of CoMoCat-SWNTs spin-coated from 1,2-dichlorobenzene onto prepatterned gold electrodes. (B) Determination of work function of plasma-cleaned gold and thin films of CoMoCat-SWNTs by photoemission yield spectroscopy. Transfer (C,D) and output characteristics (E,F) of FETs with gold electrodes with spin-coated SWNTs and pure F8BT film ($L$ = 20 $\mu$m, $W/L$ = 1000, $C_i$ = 4.4 nF cm$^{-2}$).**

electrons using low work function electrodes (calcium) that are not stable in air.[28]

Using SWNTs as additives to the semiconducting polymer layer or as surface modification of the injecting electrodes of polymer FETs substantially enhances the performance of these devices. In order to be able to maximize this improvement or to use this method in a wider range of devices, it is vital to understand the mechanism of the injection enhancement. One possible reason for the reduced contact resistance for electron and hole injection in FETs with SWNT electrodes and in polymer/SWNT blend devices could be the different work function of carbon nanotubes compared to gold. To test this hypothesis, we determined the work function of plasma-cleaned gold as used in our standard devices and the work function/ionization potential of spin-cast semiconducting carbon nanotubes (CoMoCat) by photoemission yield spectroscopy in air. The results are shown in Figure 5B. The work function of freshly plasma-cleaned gold was 5.3 eV and that of the SWNT thin films on gold and on glass was 4.9 eV. This reduction compared to gold could possibly explain the improved electron injection in a stepwise injection process from the gold to the nanotubes into the polymer, but not the improvement of hole injection, as such a work function shift would increase the energy barrier with respect to the HOMO of F8BT and F8. The conclusion that the change of the effective electrode work function cannot be responsible for the contact resistance reduction is corroborated by the experimental energy levels of semiconducting carbon nanotubes as determined by Tanaka *et al.*[32] compared to F8BT and F8, as shown for a (7,5) nanotube in Figure 1B. The highest occupied van Hove singularities range from 5.0 to 4.8 eV and the lowest unoccupied von Hove singularities from 3.9 to 4.1 eV for semiconducting HipCO SWNTs dispersed by F8BT and F8. They would thus have some effect on the injection of electrons and essentially no effect on the injection of holes into either polymer.

Another possible mechanism for improved injection along the lines of reduced injection barriers is the possible hybridization of energy levels and $\pi-\pi$ stacking between the polymer and the carbon nanotubes. Evaluation of this concept requires quantum mechanical calculations of the energy levels of the polymer wrapped around the nanotubes depending on their chirality and the specific polymer. These are currently not available. We also assume that possible effects would depend on the charge carrier type and specific nanotube, which does not seem to play a role here.

The excellent properties of FETs with spin-coated SWNTs on their source/drain electrodes might suggest that the improved device characteristics of the blend devices are due to a vertical phase separation that could lead to an enrichment of nanotubes at the contacts. However, as shown in Figure S4, reduced onset voltages and enhanced ambipolar currents are also evident for FETs with inverted (flipped) F8BT/HipCO films. These were spin-cast onto mica substrates,

floated off in water, and transferred upside down onto a substrate with prepatterned gold source–drain electrodes. The observation that devices with flipped and not flipped (but also floated off) films show the same performance strongly indicates that no segregation of SWNTs at the interface takes place.

We can thus assume that most nanotubes (probably 50 nm to 1 $\mu$m long) are randomly distributed in the polymer film, but with a preferential orientation parallel to the substrate similar to the polymer due to the strong shear forces during spin-coating. Possible tilt angles are expected to be less than 10°. This can be estimated by considering that the devices are not shorting to the gate, which would be caused by nanotubes poking out of the semiconducting film. This possibility was also excluded by atomic force microscopy of the top and bottom surface of the polymer films. Rejecting the energy levels of the SWNTs as the main reason for injection enhancement, two other mechanisms seem likely to play an important role.

First, SWNTs can reduce the vertical bulk resistance of the polymer film, which is a significant part of the overall contact resistance in bottom contact/top gate FETs,[33] particularly when the organic semiconductor exhibits a poor intrinsic conductivity as in the case of F8BT and F8.[10,11,34] To investigate the influence of the SWNTs mixed into the F8BT film, we compared a set of F8BT/HipCO FETs with different film thicknesses to pure F8BT devices with identical film thicknesses (S5). Figure S5A,B shows that, without nanotubes, the onset voltage in the output curves for holes and electrons (defined as the drain voltage at which the current starts to rise and which is indicative of the overall non-ohmic contact resistance) increases significantly with film thickness. However, this is not observed for the FETs with F8BT/SWNT blends. Figure S5C,D shows that the onset voltages essentially remain constant with increasing film thickness and the currents even improve slightly. This would mean that the contact resistance remains approximately constant despite the thicker polymer layer. Given that the contribution by the injection barrier remains unaltered (except for the linear change of the effective gate field), this means that the bulk resistance stays almost constant. Since the number of F8BT molecules, to and from which a hole or electron needs to hop, is proportional to the layer thickness, the bulk resistance can only stay constant if charges are injected into the nanotubes and are transported through them toward the interface with the PMMA dielectric and thus the conduction channel. This is certainly possible even with very few nanotubes considering their average length $l$ and possible tilt angles $\alpha$, as illustrated in Figure 6A. The conductivity of a semiconducting nanotube ($\sim$1 S·cm$^{-1}$)[35] is more than 10 orders of magnitude higher than that of the undoped polymer ($\sim 1 \times 10^{-10}$ S·cm$^{-1}$),[34] and they can carry extremely high currents. Although it is

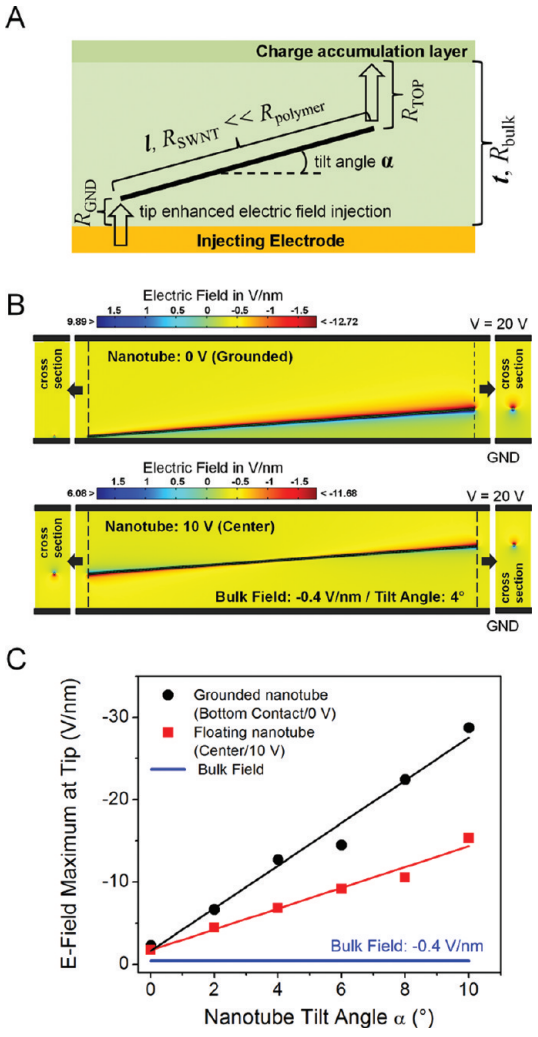


**Figure 6. (A) Schematic illustration of reduced bulk resistance and enhanced vertical electric field in a polymer layer with thickness *t*, containing a nanotube with length *l*, tilted at an angle α. (B) Simulations of enhanced electric field at and in the vicinity of a tilted (α = 4°) nanotube at ground potential or at 10 V. (C) Dependence of maximum electric field at the nanotube tip on tilt angle compared to the bulk electric field of −0.4 V/nm.**

unlikely that a nanotube bridges the entire distance $t$ between injecting electrode and charge accumulation layer, it would still result in a significant reduction of the bulk resistance $R_{bulk}$. Due to the much lower intrinsic resistivity of the SWNT, effectively only a reduced thickness of $t - (l \times \sin \alpha)$ of the high resistivity polymer needs to be overcome by a charge carrier. This reduction of the bulk resistance scales linearly with $\alpha$ for small tilt angles. The fact that the contact resistance of FETs with SWNT/polymer blends remains constant for increasing film thicknesses may indicate that the nanotubes reduce the effective bulk polymer resistance substantially and independently of the carrier polarity.

A second possible mechanism explaining the improved charge injection for both holes and electrons is due to the one-dimensional shape of the integrated SWNTs.

The vertical electric field is enhanced locally around the SWNTs, in particular at their tips. This effect has been reported to lead to improved charge injection in coplanar FETs with nanotubes extending laterally from the electrodes into the channel.[18,36] However, we are specifically looking at the vertical field and include nanotubes that are not in contact with the electrodes. The field enhancement with nanotubes for small tilt angles can be simulated using COMSOL Multiphysics software in a simple dc field dielectric configuration (disregarding current flow and charge accumulation that could lead to screening effects). The results are shown in Figure 6B and S6 for the example of a tilt angle of 4° and a nominal vertical electric field of ~0.4 V/nm (or 20 V over 50 nm of polymer). Two different cases are distinguished, depending on whether the nanotube is touching the injecting bottom electrode (*i.e.*, grounded) or whether the nanotube is embedded within the polymer matrix (*i.e.*, floating). The maximum fields at the tip of the nanotube *versus* the tilt angle are plotted in Figure 6C. In both cases, there are substantially higher fields at the nanotube tips, with field enhancement of 1−2 orders of magnitude increasing linearly with the tilt angle. However, even when the nanotube is not tilted at all, a field enhancement of a factor of 2 persists. Most injection mechanisms proposed for charge injection into organic semiconductors, such as diffusion-limited thermionic emission or thermally assisted tunneling into localized states, show a power law or even exponential dependence on the applied field.[37,38] Thus an increase of the field strength by an order of magnitude due to the presence of the SWNTs in the vicinity of the injecting electrodes enhances the injection efficiency disproportionately and hence lowers the total contact resistance dramatically. For FETs with thicker polymer films, the nanotubes are more likely to adopt steeper tilt angles than for thin films due to the different viscosities of the polymer solutions and fewer space restrictions. A larger tilt angle will increase the field enhancement at the tips, and thus a good injection would be expected even for thicker polymer films, as seen in Figure S5. Unfortunately, determining the exact vertical position and orientation of the nanotubes within a conjugated polymer film was not possible with the currently available experimental methods.

Both of the above proposed mechanisms can explain the apparently even further reduced contact resistances in the case of SWNT-coated gold electrodes. When the pure polymer is spun on top and infiltrates the dense SWNT network, more interconnected nanotube pathways between the electrode and the accumulation layer become available, which lowers the bulk resistance. Equally, the density of nanotube tips and thus sites for field enhancement is increased drastically, as well. In conclusion, both mechanisms are likely to play a role, but the localized field enhancement is probably dominant due to the nonlinear dependence of charge injection on the electric field.

As both mechanisms are independent of the polarity of the injected charge carrier and applicable for all types of bottom contact/top gate FETs using polymer semiconductors, this method could be applied to improve device characteristics where efficient charge injection is an issue. For example, LEFETs that need a thick semiconducting layer for the incorporation of waveguides would benefit from low contact resistance independent of film thickness. The type of SWNT (metallic or semiconducting) is not a major concern, and the concentration of SWNTs can easily be reduced below the percolation limit by dilution so that most conjugated polymers could be used, as well.

In summary, we improved the device characteristics of ambipolar field-effect transistors in a bottom contact/top gate geometry based on the conjugated polymers F8BT and F8 by adding small amounts of SWNTs to the semiconducting polymer layer. The threshold/onset voltages for both holes and electrons were lowered, and substantially diminished contact resistances were achieved. Consequently, ambipolar currents and maximum light emission intensities were 1−2 orders of magnitude higher than in devices without nanotubes. An even stronger positive effect was observed for devices with gold electrodes coated with a dense SWNT layer. We conclude that energy level alignment at the electrode/semiconductor interface cannot be the main cause of the observed improvements. Instead, we find that a combined reduction of the bulk resistance by the highly conductive SWNTs and enhancement of the local electric field at the SWNT tips and thus increased injection efficiency are the most likely causes. We believe that this simple method of blending organic semiconductor films with small amounts of SWNTs can be of great use, not only for ambipolar LEFETs but also for many organic optoelectronic devices suffering from injection barriers and high contact resistance in general.

## METHODS

**Polymer/Nanotube Dispersion Preparation.** The conjugated polymers used in this study, poly(9,9-dioctylfluorenyl-2,7-diyl) (F8, $M_n$ = 110 kg·mol$^{-1}$, PD = 2.4) and poly[(9,9-dioctylfluorenyl-2,7-diyl)-*alt*-*co*-(1,4-benzo-2,1′,3-thiadiazole)] (F8BT, $M_n$ = 61 kg·mol$^{-1}$, PD = 3.1), were supplied by Cambridge Display Technology Ltd. Single-walled carbon nanotubes produced by the HipCO process (diameter 0.8−1.2 nm, purified <13 wt % iron) were purchased from Unidym Inc. Polymer solutions (2 mg/mL in *o*-xylene, anhydrous, Sigma-Aldrich) were heated for 30 min at 70 °C to remove aggregates, which can affect dispersion. After

cooling, the nanotube powder was added at 2 mg/mL, and dispersions were homogenized in an ultrasonic bath for 60 min, followed by vigorous sonication using a tip sonicator (Sonics Vibra Cell) for 10 min to induce debundling. After centrifugation at 60 000*g* for 30 min (Beckman Coulter Avanti J26XP), the supernatant was collected. Note, the polymer concentration in solution is reduced by about 50% after centrifugation, as determined by absorption spectroscopy. In addition, ultrasonication of the polymer solutions reduces the average molar mass by 12−32% (see Figure S1). Molar mass distributions were determined by gel permeation chromatography with the polymer dissolved in tetrahydrofuran (1 mg/mL). Characterization of the polymer−nanotube dispersion was carried out with a Cary 6000i UV/vis/NIR absorption spectrometer (Varian), and excitation−emission maps were collected with a Horiba Scientific Fluorolog-3 with an InGaAs diode array detector. All processing and characterization steps were carried out under ambient conditions.

**Fabrication of Field-Effect Transistors.** Low-sodium Schott AF 32 eco glass served as a substrate for field-effect transistors. Interdigitated source/drain electrodes were patterned by photolithography, thermal evaporation of 1 nm chromium and 30 nm gold, and lift-off (channel width $W$ = 20 mm, channel length $L$ = 20 $\mu$m). The substrates and electrodes were cleaned with oxygen plasma (250 W, 10 min). The total polymer concentration was adjusted to 6 mg/mL for regular F8 and F8BT solutions to give a film thickness of 40−60 nm after spin-coating. For thickness-dependent measurements, polymer solutions of 7, 11, and 13.5 mg/mL (39, 75, and 135 nm) were prepared from a polymer/SWNT stock dispersion in order to achieve a constant nanotube to polymer weight ratio. Subsequent annealing above $T_M$ at 290 °C (30 min) or below $T_G$ at 120 °C (60 min) removed residual solvent and moisture. Annealing above the liquid crystalline melt induced polycrystallinity. Spin-coating PMMA (Polymer Source Inc., $M_w$ = 319 kg·mol$^{-1}$, PD = 1.25) from filtered anhydrous *n*-butylacetate solution (60 mg/mL) on top of the semiconducting film formed the dielectric layer (approximately 500 nm). Evaporation of 15 nm of gold through a shadow mask as a gate electrode completed the FET. Reference samples without nanotubes were processed in the same way only without nanotubes. All spin-coating and annealing steps were carried out in a nitrogen glovebox.

Field-effect transistors with Au/SWNT electrodes were fabricated by spin-coating purified CoMoCat carbon nanotubes (>90% semiconducting SWNT, Southwest Nanotechnology) from 1,2-dichlorobenzene dispersions onto prepatterned gold electrodes. Photolithography with an identical but inverse photomask protected the nanotubes on the electrodes with photoresist, while those in the channel region were exposed and completely removed by oxygen plasma. After removal of the photoresist, all FETs were completed as described above but with pure F8BT solutions (7 mg/mL in *o*-xylene). The work function/ionization potential of CoMoCat-SWNT thin films compared to clean gold was determined by photoemission yield spectroscopy in air (AC-2, RIKEN KEIKI CO., LTD).

**Device Characterization.** Electrical and optical device characterization was carried out in nitrogen atmosphere with an Agilent 4155C semiconductor parameter analyzer and a Hamamatsu S1133-01 silicon photodiode. For photocurrent measurements, the photodiode was biased at −3 V and placed directly on top of the FET. Capacitance measurements of the dielectric layer for mobility calculations were performed on 1 × 1 mm contact pads with a HP4192A impedance analyzer.

**Simulations.** Electrostatic conditions at the nanotube were simulated with COMSOL Multiphysics to investigate the electric field distribution between ground (0 V) and a virtual top electrode (20 V) to represent the gate field. The nanotube (length = 200 nm, diameter = 1 nm) with an estimated conductivity of about 1 S·cm$^{-1}$ exceeds the conductivity of undoped F8BT (1 × 10$^{-10}$ S·cm$^{-1}$) by several orders of magnitude. Consequently, a homogeneous potential was assumed within the nanotube, which is determined by the nanotube position within the polymer film acting as a voltage divider, that is, all voltage drops across the polymer between nanotube and adjacent electrode. For calculations of the maximum electric field, the nanotube was either in contact with ground (0 V) or placed in the channel center (10 V). The simulation was carried out as purely dielectric, no current flow or charge density was included. See also Supporting Information S6.

*Acknowledgment.* The authors thank Cambridge Display Technologies Ltd. for the generous supply of the conjugated polymers (F8 and F8BT) and photoemission yield spectroscopy measurements. M.C.G. acknowledges support by the Gates Cambridge Trust. J.Z. and F.J. acknowledge financial support by the Deutsche Forschungsgemeinschaft (DFG ZA 638/3), Excellence Cluster "Engineering of Advanced Materials" (EXC 315), and the Alfried Krupp von Bohlen und Halbach Foundation. The authors thank C. Backes, J. Englert, and F. Hauke (Institute of Advanced Materials and Processes (ZMP), University of Erlangen-Nuremberg) for help with excitation−emission map measurements, M. Malter for GPC measurements, and F. Bonaccorso (Centre for Advanced Photonics and Electronics (CAPE), University of Cambridge) for early discussions.

*Supporting Information Available:* Molar mass distributions of the used polymers before and after sonication, gated four-point probe contact resistance measurements, additional current−voltage characteristics of FETs with flipped polymer films, F8BT annealed below the glass transition temperature and for different film thicknesses, and further information on electric field distribution simulations. This material is available free of charge *via* the Internet at http://pubs.acs.org.

## REFERENCES AND NOTES

1. Ishii, H.; Sugiyama, K.; Ito, E.; Seki, K. Energy Level Alignment and Interfacial Electronic Structures at Organic Metal and Organic Organic Interfaces. *Adv. Mater.* **1999**, *11*, 605–625.
2. Kahn, A.; Koch, N.; Gao, W. Electronic Structure and Electrical Properties of Interfaces between Metals and $\pi$-Conjugated Molecular Films. *J. Polym. Sci., Part B: Polym. Phys.* **2003**, *41*, 2529–2548.
3. Anthopoulos, T. D.; Setayesh, S.; Smits, E.; Colle, M.; Cantatore, E.; de Boer, B.; Blom, P. W. M.; de Leeuw, D. M. Air-Stable Complementary-like Circuits Based on Organic Ambipolar Transistors. *Adv. Mater.* **2006**, *18*, 1900–1904.
4. Zaumseil, J.; Sirringhaus, H. Electron and Ambipolar Transport in Organic Field-Effect Transistors. *Chem. Rev.* **2007**, *107*, 1296–1323.
5. Swensen, J. S.; Soci, C.; Heeger, A. J. Light Emission from an Ambipolar Semiconducting Polymer Field-Effect Transistor. *Appl. Phys. Lett.* **2005**, *87*, 253511.
6. Zaumseil, J.; Friend, R. H.; Sirringhaus, H. Spatial Control of the Recombination Zone in an Ambipolar Light-Emitting Organic Transistor. *Nat. Mater.* **2006**, *5*, 69–74.
7. Gwinner, M. C.; Vaynzof, Y.; Banger, K. K.; Ho, P. K. H.; Friend, R. H.; Sirringhaus, H. Solution-Processed Zinc Oxide as High-Performance Air-Stable Electron Injector in Organic Ambipolar Light-Emitting Field-Effect Transistors. *Adv. Funct. Mater.* **2010**, *20*, 3457–3465.
8. Khodabakhsh, S.; Poplavskyy, D.; Heutz, S.; Nelson, J.; Bradley, D. D. C.; Murata, H.; Jones, T. S. Using Self-Assembling Dipole Molecules To Improve Hole Injection in Conjugated Polymers. *Adv. Funct. Mater.* **2004**, *14*, 1205–1210.
9. de Boer, B.; Hadipour, A.; Mandoc, M. M.; van Woudenbergh, T.; Blom, P. W. M. Tuning of Metal Work Functions with Self-Assembled Monolayers. *Adv. Mater.* **2005**, *17*, 621–625.
10. Cheng, X. Y.; Noh, Y. Y.; Wang, J. P.; Tello, M.; Frisch, J.; Blum, R. P.; Vollmer, A.; Rabe, J. P.; Koch, N.; Sirringhaus, H. Controlling Electron and Hole Charge Injection in Ambipolar Organic Field-Effect Transistors by Self-Assembled Monolayers. *Adv. Funct. Mater.* **2009**, *19*, 2407–2415.
11. Gwinner, M. C.; Khodabakhsh, S.; Giessen, H.; Sirringhaus, H. Simultaneous Optimization of Light Gain and Charge Transport in Ambipolar Light-Emitting Polymer Field-Effect Transistors. *Chem. Mater.* **2009**, *21*, 4425–4433.

12. Hill, I. G. Numerical Simulations of Contact Resistance in Organic Thin-Film Transistors. *Appl. Phys. Lett.* **2005**, *87*, 163505.
13. Street, R. A.; Salleo, A. Contact Effects in Polymer Transistors. *Appl. Phys. Lett.* **2002**, *81*, 2887–2889.
14. Richards, T. J.; Sirringhaus, H. Analysis of the Contact Resistance in Staggered, Top-Gate Organic Field-Effect Transistors. *J. Appl. Phys.* **2007**, *102*, 094510.
15. Zaumseil, J.; Donley, C. L.; Kim, J. S.; Friend, R. H.; Sirringhaus, H. Efficient Top-Gate, Ambipolar, Light-Emitting Field-Effect Transistors Based on a Green-Light-Emitting Polyfluorene. *Adv. Mater.* **2006**, *18*, 2708–2712.
16. Zaumseil, J.; McNeill, C. R.; Bird, M.; Smith, D. L.; Ruden, P. P.; Roberts, M.; McKiernan, M. J.; Friend, R. H.; Sirringhaus, H. Quantum Efficiency of Ambipolar Light-Emitting Polymer Field-Effect Transistors. *J. Appl. Phys.* **2008**, *103*, 064517.
17. Aguirre, C. M.; Ternon, C.; Paillet, M.; Desjardins, P.; Martel, R. Carbon Nanotubes as Injection Electrodes for Organic Thin Film Transistors. *Nano Lett.* **2009**, *9*, 1457–1461.
18. Cicoira, F.; Aguirre, C. M.; Martel, R. Making Contacts to n-Type Organic Transistors Using Carbon Nanotube Arrays. *ACS Nano* **2011**, *5*, 283–290.
19. Lefenfeld, M.; Blanchet, G.; Rogers, J. A. High-Performance Contacts in Plastic Transistors and Logic Gates That Use Printed Electrodes of DNNSA-PANI Doped with Single-Walled Carbon Nanotubes. *Adv. Mater.* **2003**, *15*, 1188–1191.
20. Southard, A.; Sangwan, V.; Cheng, J.; Williams, E. D.; Fuhrer, M. S. Solution-Processed Single Walled Carbon Nanotube Electrodes for Organic Thin-Film Transistors. *Org. Electron.* **2009**, *10*, 1556–1561.
21. Hellstrom, S. L.; Jin, R. Z.; Stoltenberg, R. M.; Bao, Z. Driving High-Performance n- and p-Type Organic Transistors with Carbon Nanotube/Conjugated Polymer Composite Electrodes Patterned Directly from Solution. *Adv. Mater.* **2010**, *22*, 4204–4208.
22. McCarthy, M. A.; Liu, B.; Rinzler, A. G. High Current, Low Voltage Carbon Nanotube Enabled Vertical Organic Field Effect Transistors. *Nano Lett.* **2010**, *10*, 3467–3472.
23. McCarthy, M. A.; Liu, B.; Donoghue, E. P.; Kravchenko, I.; Kim, D. Y.; So, F.; Rinzler, A. G. Low-Voltage, Low-Power, Organic Light-Emitting Transistors for Active Matrix Displays. *Science* **2011**, *332*, 570–573.
24. Kymakis, E.; Amaratunga, G. A. J. Single-Wall Carbon Nanotube/Conjugated Polymer Photovoltaic Devices. *Appl. Phys. Lett.* **2002**, *80*, 112–114.
25. Arranz-Andrés, J.; Blau, W. J. Enhanced Device Performance Using Different Carbon Nanotube Types in Polymer Photovoltaic Devices. *Carbon* **2008**, *46*, 2067–2075.
26. Nish, A.; Hwang, J. Y.; Doig, J.; Nicholas, R. J. Highly Selective Dispersion of Single-Walled Carbon Nanotubes Using Aromatic Polymers. *Nat. Nanotechnol.* **2007**, *2*, 640–646.
27. Chen, F. M.; Wang, B.; Chen, Y.; Li, L. J. Toward the Extraction of Single Species of Single-Walled Carbon Nanotubes Using Fluorene-Based Polymers. *Nano Lett.* **2007**, *7*, 3013–3017.
28. Donley, C. L.; Zaumseil, J.; Andreasen, J. W.; Nielsen, M. M.; Sirringhaus, H.; Friend, R. H.; Kim, J. S. Effects of Packing Structure on the Optoelectronic and Charge Transport Properties in Poly(9,9-di-*n*-octylfluorene-*alt*-benzothiadiazole). *J. Am. Chem. Soc.* **2005**, *127*, 12890–12899.
29. Schöppler, F.; Mann, C.; Hain, T. C.; Neubauer, F. M.; Privitera, G.; Bonaccorso, F.; Chu, D.; Ferrari, A. C.; Hertel, T. Molar Extinction Coefficient of Single-Wall Carbon Nanotubes. *J. Phys. Chem. C* **2011**, *115*, 14682–14686.
30. Nish, A.; Hwang, J. Y.; Doig, J.; Nicholas, R. J. Direct Spectroscopic Evidence of Energy Transfer from Photo-excited Semiconducting Polymers to Single-Walled Carbon Nanotubes. *Nanotechnology* **2008**, *19*, 095603.
31. Gwinner, M. C.; Khodabakhsh, S.; Song, M. H.; Schweizer, H.; Giessen, H.; Sirringhaus, H. Integration of a Rib Waveguide Distributed Feedback Structure into a Light-Emitting Polymer Field-Effect Transistor. *Adv. Funct. Mater.* **2009**, *19*, 1360–1370.
32. Tanaka, Y.; Hirana, Y.; Niidome, Y.; Kato, K.; Saito, S.; Nakashima, N. Experimentally Determined Redox Potentials of Individual (*n*,*m*) Single-Walled Carbon Nanotubes. *Angew. Chem., Int. Ed.* **2009**, *48*, 7655–7659.
33. Burgi, L.; Richards, T. J.; Friend, R. H.; Sirringhaus, H. Close Look at Charge Carrier Injection in Polymer Field-Effect Transistors. *J. Appl. Phys.* **2003**, *94*, 6129–6137.
34. Yim, K.-H.; Whiting, G. L.; Murphy, C. E.; Halls, J. J. M.; Burroughes, J. H.; Friend, R. H.; Kim, J.-S. Controlling Electrical Properties of Conjugated Polymers *via* a Solution-Based p-Type Doping. *Adv. Mater.* **2008**, *20*, 3319–3324.
35. Zhou, X. J.; Park, J. Y.; Huang, S. M.; Liu, J.; McEuen, P. L. Band Structure, Phonon Scattering, and the Performance Limit of Single-Walled Carbon Nanotube Transistors. *Phys. Rev. Lett.* **2005**, *95*, 146805.
36. Cicoira, F.; Coppede, N.; Iannotta, S.; Martel, R. Ambipolar Copper Phthalocyanine Transistors with Carbon Nanotube Array Electrodes. *Appl. Phys. Lett.* **2011**, *98*, 183303.
37. Scott, J. C. Metal–Organic Interface and Charge Injection in Organic Electronic Devices. *J. Vac. Sci. Technol., A* **2003**, *21*, 521–531.
38. Ng, T. N.; Silveira, W. R.; Marohn, J. A. Dependence of Charge Injection on Temperature, Electric Field, and Energetic Disorder in an Organic Semiconductor. *Phys. Rev. Lett.* **2007**, *98*, 066101.